Desalination and Water Treatment
www.deswater.com

doi: 10.5004/dwt.2018.21718

101 (2018) 178–184
January

Broad-spectrum adsorbent of cations derived from methacrylic-acid-modified rice husk

Wen-Feng Hsiao[a], Shih-Tong Hsu[b], Ting-Chung Pan[c,*], Ren-Hao Tsai[c], Cheng-Jui Lin[c]

[a]*Department of Plant Medicine, National Chiayi University, No. 300 Syuefu Rd., Chiayi City 60004, Taiwan, email: wfhsiao@mail.ncyu.edu.tw*
[b]*Department of Materials Engineering, Kun Shan University, No. 195, Kunda Rd., Yong-Kang Dist., Tainan City 71003, Taiwan, email: shihtong@mail.ksu.edu.tw*
[c]*Department of Environmental Engineering, Kun Shan University, No. 195, Kunda Rd., Yong-Kang Dist., Tainan City 71003, Taiwan, Tel. +886 6 2050443; Fax: +886 6 2050540; emails: tcpan@mail.ksu.edu.tw (T.-C. Pan), renhao791202@gmail.com (R.-H. Tsai), applelin310@yahoo.com.tw (C.-J. Lin)*

Received 3 June 2017; Accepted 21 November 2017

ABSTRACT

Polymethacrylic acid (PMAA) grafted rice husk (rh) was prepared using graft copolymerization and applied to the adsorption of several cations in water solution. The grafted copolymer was characterized in terms of Barrett–Emmett–Teller specific surface area and Fourier-transform infrared spectroscopy to measure the specific surface area and functional groups of the rh before and after chemical modification. A representative polymethacrylic-acid-grafted rice husk (rh-*g*-PMAA) copolymer was neutralized to a salt type (rh-*g*-PMANa) and applied to the adsorption of $Pb^{2+}_{(aq)}$, $Cu^{2+}_{(aq)}$, NH_4^+–N, methyl violet, and malachite green. The maximum adsorption capacities of these cations were 332.0, 134.7, 33.67, 360.7, and 232.8 mg/g-adsorbent, respectively. These values are higher than those for many common binding agents used for the tested cations. The adsorption equilibrium data correlate more closely with Langmuir isotherms than with Freundlich isotherms, except that for NH_4^+–N.

Keywords: Adsorbent; Cation; Methacrylic acid; Rice husk

1. Introduction

In the goal of environmental protection, wastewater treatment is one of the most important topics. Pollutants in wastewater include cations, anions, and nonionic materials from the occupied charge point of view. Many methods can be used to remove those substances, such as precipitation, oxidation by ozone [1], ion exchange [2], membrane adsorbent [3] adsorption, and so on. Adsorption technology is used extensively for the removal of solutes dissolved in aqueous solutions. Activated carbon (AC) is the most versatile adsorbent for the removal of pollutants in wastewater [4,5]. AC can be produced in numerous ways. Recently, AC has been produced from various waste biomass sources [6,7], prepared from waste materials using the microwave heating method [8], and combined with other processes to increase performance [9,10]. The high cost and energy consumption of AC production are important challenges for commercial manufacturers. The preparation of low-cost adsorbents from waste materials has several advantages, mainly economic and environmental. A wide variety of low-cost adsorbents have been prepared from various waste materials, such as agricultural, industrial, and municipal waste [11–14]. A relatively good adsorption capacity for pollutants is the major target for new adsorbents.

In the present work, a broad-spectrum adsorbent of cations is proposed. It is produced from polymethacrylic-acid-modified rice husk (rh-*g*-PMAA) via graft

* Corresponding author.

copolymerization using Fenton's reagent as a redox initiator [15]. rh-*g*-PMAA with a grafting percentage of 66.7% ± 2.0% was neutralized to a sodium salt type (rh-*g*-PMANa). Its preparation was a 1-h reaction at 82°C. Separation of the graft copolymer product and the reaction solution was only used to precipitate by gravitation. The adsorbent rh-*g*-PMANa is more environmentally friendly than AC. rh-*g*-PMANa was used to adsorb several types of cationic pollutant, namely $Pb^{2+}_{(aq)}$, $Cu^{2+}_{(aq)}$, NH_4^+–N, malachite green (MG), and methyl violet (MV) in water solution. $Pb^{2+}_{(aq)}$ and $Cu^{2+}_{(aq)}$ are heavy metals that are toxic to humans and other organisms, and thus it is extremely important to remove them from wastewater [16,17]. The presence of a large amount of NH_4^+–N in lakes, slow-flowing rivers, and gulfs can cause eutrophication, which leads to foul odors and low dissolved oxygen content for aquatic species [18,19]. MV is a triphenylmethane dye that may cause severe skin, eye, and respiratory tract irritation [20]. It increases the organic content in the wastewater of textile and printing industries. MG is a cationic dye that is widely used as a fungicide in the aquaculture industry to control fish parasites. It has been found to exhibit carcinogenic, genotoxic, and mutagenic properties [21,22]. Although the removal of MV and MG by AC is effective and efficient [23,24], a new adsorbent for these compounds would be valuable. A short summary of the adsorption results for the $Pb^{2+}_{(aq)}$, $Cu^{2+}_{(aq)}$, NH_4^+–N, MV, and MG is listed in Table 1.

2. Experiments

2.1. Materials

Original rice husk (rh) was obtained from a local rice mill in southern Taiwan. It was treated with a diluted NaOH aqueous solution to eliminate trace organic residues and washed with distilled water to a pH of 7.0. The clean rh was dried at 50°C in an oven until a constant weight was achieved. Methacrylic acid, ferrous ammonium sulfate, hydrogen peroxide, ammonium chloride, copper nitrate, lead nitrate, MV, MC, and acetone were analytical grade or better and used without further purification.

2.2. Preparation of adsorbent

A graft copolymer of methacrylic acid and rh (rh-*g*-PMAA) was synthesized via graft copolymerization. The optimal copolymerization conditions, determined using central composite design, were an $Fe^{2+}_{(aq)}$ concentration of 0.5×10^{-3} M, an H_2O_2 concentration of 0.14 M, and a temperature of 82.0°C. Grafting percentages of the products were 66.7% ± 2.0% [15].

rh-*g*-PMAA was added to a conical flask that contained 0.1 M aqueous NaOH. The solution was stirred for 1 h before being filtered and washed in distilled water until it became a neutralized filter liquor. It was then dried at 50°C under vacuum. The neutralized product was the sodium salt of rh-*g*-PMAA (rh-*g*-PMANa).

2.3. Characterization of adsorbent

The specific surface areas of the powder samples were determined using the Barrett–Emmett–Teller (BET) approach using a Micromeritics ASAP 2020 apparatus. The measurements of BET surface area were made at 50°C/1 h/15 μmHg (Degas 1) and 60°C/2 h (Degas 2). Fourier-transform infrared (FTIR) analysis of the copolymer samples was performed using a PerkinElmer FT-IR spectrometer in the wavenumber range of 4,000–400 cm^{-1}.

Table 1
The results of various reported studies on the adsorption of $Pb^{2+}_{(aq)}$, $Cu^{2+}_{(aq)}$, NH_4^+–N, methyl violet, and malachite green by various adsorbents

Cationic material	Adsorbents	Monolayer capacity, q_m mg/g-adsorbent	References
$Pb^{2+}_{(aq)}$	Iron oxide nanoparticles and *A. fabrum* strains encapsulated in calcium alginate	197.02	[26]
	Amylopectin-*g*-poly(acrylamide-*co*-acrylic acid)	51.8	[27]
$Cu^{2+}_{(aq)}$	Composite electrospun cellulose acetate/titanium oxide (TiO_2)	23	[28]
	$Bi_2Fe_4O_9$ nanoplate	42.7	[29]
	Polyethylenimine-modified polystyrene/Fe_3O_4/chitosan magnetic composites	204.6	[30]
NH_4^+–N	Clinoptilolite	10.80	[31]
	Biochar produced from oak sawdust	4.13	[32]
	Palygorskite nanocomposite	237.6	[33]
Methyl violet	Nanostructured carbon covered sand	49.03	[34]
	Granulated mesoporous carbon	202.8	[35]
	Palygorskite	218.11	[36]
Malachite green	Copper oxide nanoparticle-loaded activated carbon	87.719	[37]
	Organically modified hydroxyapatite	188.18	[38]
	Tetraethylenepentamine functionalized activated carbon	333.3	[39]
	Magnetic hydroxyapatite nanopowder	526	[40]

2.4. Adsorption of cations in aqueous solution

Adsorption experiments were carried out in a 1-L resin kettle at 37.5°C for 2 h. The agitation rate was controlled to be around 600 rpm to avoid the liquid film diffusion resistance. The adsorption solution comprised 0.2 g of rh-*g*-PMANa adsorbent sieved from 10 to 40 meshes. The pH values of adsorption solutions were 4.60 ± 0.60 for $Pb^{2+}_{(aq)}$, $Cu^{2+}_{(aq)}$, MV, and MG and 9.50 ± 0.20 for NH_4^+–N without the use of a chemical reagent. Each sample (0.2 mL) was taken using a micropipette at various times to measure the concentration of cations.

2.4.1. Adsorption of $Pb^{2+}_{(aq)}$ and $Cu^{2+}_{(aq)}$

The $Pb^{2+}_{(aq)}$ ion samples, taken at various time, were analyzed by PerkinElmer AA-200 atomic absorption spectrometer. The adsorption amount (q_e) was calculated as:

$$q_e = (C_0 - C_e)V/m \quad (1)$$

where q_e is the amount (mg/g) of $Pb^{2+}_{(aq)}$ ions adsorbed by rh-*g*-PMANa adsorbent, C_0 and C_e are the $Pb^{2+}_{(aq)}$ ion concentrations (mg/L) in the solution initially and after adsorption, respectively, V is the volume (L) of the solution, and m is the mass (g) of adsorbent used in the experiment.

The adsorption of $Cu^{2+}_{(aq)}$ ions was calculated the same as that of $Pb^{2+}_{(aq)}$ with different initial concentrations.

2.4.2. Adsorption of NH_4^+–N, MG, and MV

The absorbance of NH_4^+–N, MG, and MV samples, taken at suitable time intervals, was measured using a Spectrumlab 22PC spectrophotometer at λ_{max} values of 425, 617, and 585 nm, respectively. The adsorption amounts (q_e) of NH_4^+–N, MG, and MV were calculated using Eq. (1).

3. Results and discussion

3.1. Preparation of the rh-g-PMANa adsorbent

Preparations of rh-*g*-PMAA copolymer were conducted as in our previous work [15]. The products were neutralized to the sodium salt of PMAA-grafted rice husk (rh-*g*-PMANa), which was used to adsorb several cations from water solution.

3.2. Characterization of synthetic adsorbent

Fig. 1(a) shows the nitrogen adsorption/desorption isotherm and Barrett–Joyner–Halenda (BJH) desorption pore size distribution curve of pure rh at 50°C. The figure includes a type IV isotherm with H1 hysteresis, which is characteristic of mesopores with capillary condensation of nitrogen in the particle matrix. The pore size is broadly distributed in the range of 2–150 nm. The same results were obtained for rh-*g*-PMAA (Fig. 1(b)) and rh-*g*-PMANa (Fig. 1(c)). The textural properties of the rh support and its derivative samples are listed in Table 2. It can be seen that the specific surface areas (S_{BET}) of rh, rh-*g*-PMAA, and rh-*g*-PMANa are 5.47, 2.23, and 1.81 $m^2\ g^{-1}$, respectively. The results indicate that the total surface areas of rh and its derivatives were very tiny

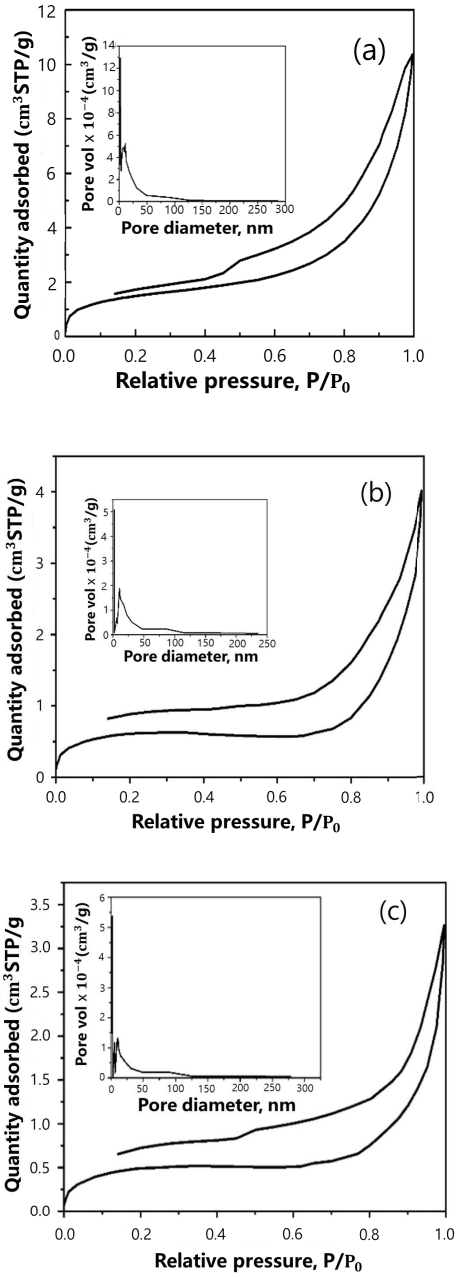

Fig. 1. Nitrogen adsorption/desorption isotherms and BJH desorption pore size distribution of (a) rh, (b) rh-*g*-PMAA, and (c) rh-*g*-PMANa.

Table 2
Specific surface area and pore properties of rice husk and its derivatives

Sample	S_{BET} ($m^2\ g^{-1}$)	Pore volume ($cm^3\ g^{-1}$)	Pore size (nm)
rh	5.47	0.016	13.63
rh-*g*-PMAA	2.23	0.0058	20.60
rh-*g*-PMANa	1.81	0.0047	20.93

compared with that of AC. The pore volumes and pore sizes were slightly decreased but not markedly different after the modification of rh.

FTIR investigations were performed to elucidate the complex interaction between rh and PMAA. Fig. 2(a) shows the spectrum of rh. The broad band at 3,414 cm^{-1} indicates the presence of OH groups on the surface molecule of rh. FTIR analysis of rh-*g*-PMAA is shown in Fig. 2(b). The peak at about 1,717 cm^{-1} is assigned to the stretching vibration of C=O from the carboxylic groups in PMAA [25]. The results reveal that the MAA monomer was grafted onto the main chain of the rh.

3.3. Adsorption of cations in aqueous solution

rh-*g*-PMAA with a grafting percentage of 66.7% ± 2.0% was neutralized to rh-*g*-PMANa and used as an adsorbent of five types of cation in water solution.

3.3.1. Adsorption of $Pb^{2+}_{(aq)}$

Fig. 3(a) plots the adsorption experiment data and the Langmuir (LM) and Freundlich (FD) correlations of $Pb^{2+}_{(aq)}$. The LM and FD isotherms and their relationship coefficients, *r*, are listed in Table 3. Since the *r* value of the LM isotherm (0.9970) is higher than that of the FD isotherm (0.9799), the LM model fitted the experimental results more closely than did the FD model. The monolayer adsorption capacity of $Pb^{2+}_{(aq)}$ calculated from the LM isotherm is 332.0 mg/g-adsorbent. This result is better than those for $Pb^{2+}_{(aq)}$ adsorbents obtained from the biosorbent-encapsulated *Agrobacterium fabrum* and iron oxide nanoparticles [26], and amylopectin-*g*-poly(acrylamide-*co*-acrylic acid) [27]. The results reveal that rh-*g*-PMANa is a potential adsorbent of $Pb^{2+}_{(aq)}$ for wastewater treatment.

3.3.2. Adsorption of $Cu^{2+}_{(aq)}$

The adsorption results of $Cu^{2+}_{(aq)}$ are plotted in Fig. 3(b). The LM and FD isotherms and relationship coefficients, *r*, are listed in Table 3. The *r* values are 0.9908 and 0.9769 for LM

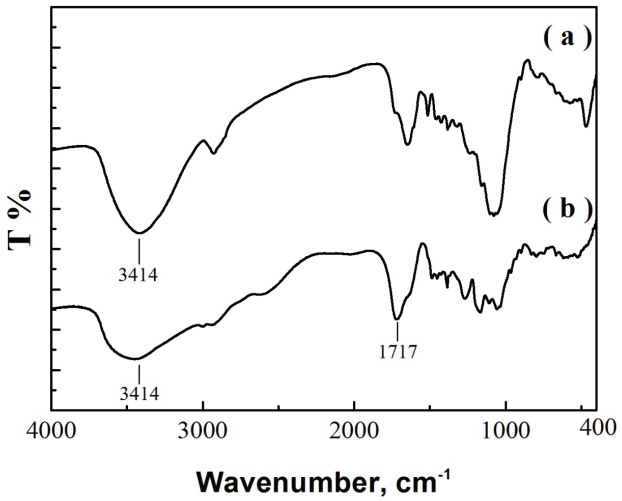

Fig. 2. FTIR spectra of (a) rh and (b) rh-*g*-PMAA.

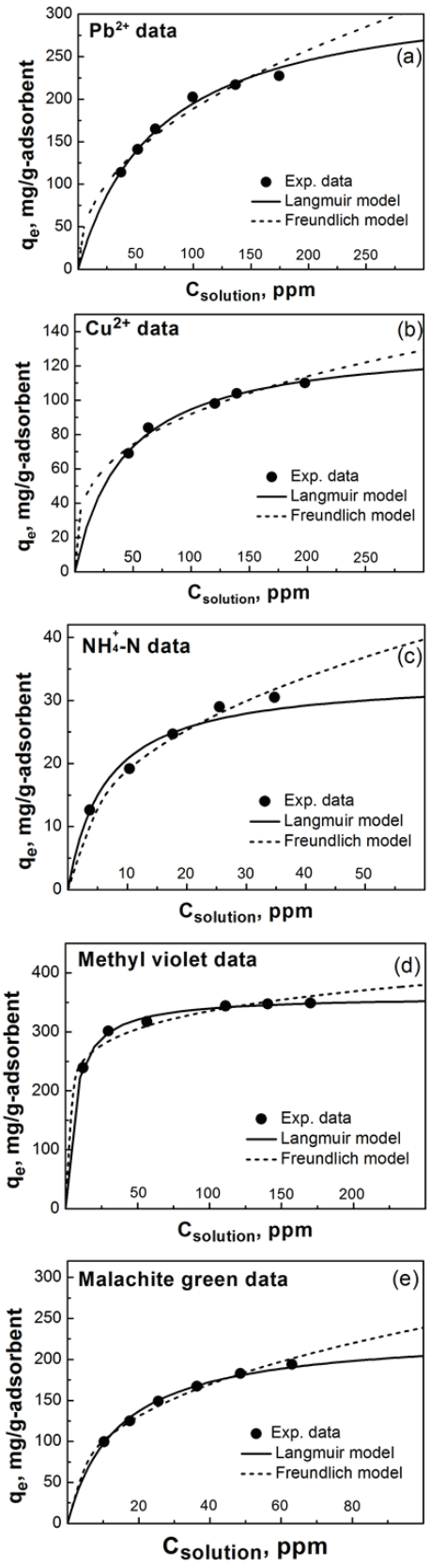

Fig. 3. LM and FD isotherms for adsorption of (a) Pb^{2+}, (b) Cu^{2+}, (c) NH_4^+–N, (d) MV, and (e) MG by rh-*g*-PMANa adsorbent.

Table 3
The Langmuir (LM) and Freundlich (FD) isotherms and relationship coefficient, *r*, of adsorption experiment

Cations	LM isotherm, monolayer adsorption capacity	*r* (LM)	FD isotherm	*r* (FD)
$Pb^{2+}_{(aq)}$	$q_e = 332.0 \times 0.01426C_e/(1 + 0.01426C_e)$ 332.0 mg/g-adsorbent	0.9970	$q_e = 3.949C_e^{1/2.217}$	0.9799
$Cu^{2+}_{(aq)}$	$q_e = 134.7 \times 0.02371C_e/(1 + 0.02371C_e)$, 134.7 mg/g-adsorbent	0.9908	$q_e = 3.839C_e^{1/3.234}$	0.9769
NH_4^+–N	$q_e = 33.67 \times 0.1690C_e/(1 + 0.1690C_e)$, 33.67 mg/g-adsorbent	0.9942	$q_e = 2.471C_e^{1/2.605}$	0.9964
MV	$q_e = 360.7 \times 0.1616C_e/(1 + 0.1616C_e)$, 360.7 mg/g-adsorbent	0.9970	$q_e = 9.505C_e^{1/7.309}$	0.9618
MG	$q_e = 232.8 \times 0.07115C_e/(1 + 0.07115C_e)$, 232.8 mg/g-adsorbent	0.9972	$q_e = 5.119C_e^{1/2.685}$	0.9938

and FD isotherms, respectively. The LM model thus fitted the experimental results more closely than did the FD model in the adsorption of $Cu^{2+}_{(aq)}$. The calculated adsorption capacity is 134.7 mg/g-adsorbent. This result is better than those for composite electrospun cellulose acetate/titanium oxide (TiO_2) adsorbent [28] and $Bi_2Fe_4O_9$ nanoplates [29], but lower than that for modified polystyrene/Fe_3O_4/chitosan magnetic composites [30]. However, rh-*g*-PMANa is still an excellent adsorbent for $Cu^{2+}_{(aq)}$ in water solution.

3.3.3. Adsorption of NH_4^+–N

Fig. 3(c) plots the adsorption experiment data and the LM and FD correlations of NH_4^+–N. The LM and FD isotherms and their relationship coefficients, *r*, are listed in Table 3. The *r* value of the FD isotherm (0.9964) is higher than that of the LM isotherm (0.9942), and thus the FD model fitted the experimental results more closely than did the LM model. The calculated monolayer adsorption capacity of NH_4^+–N is 33.67 mg/g-adsorbent. This value is higher than those for clinoptilolite [31] and modified biochar [32], but lower than that for palygorskite nanocomposite [33]. In general, rh-*g*-PMANa is a good adsorbent for NH_4^+–N in water solution.

3.3.4. Adsorption of MV

Fig. 3(d) plots the adsorption experiment data and the LM and FD correlations of MV. The LM and FD isotherms and their relationship coefficients, *r*, are listed in Table 3. The *r* values are 0.9970 and 0.9618 for LM and FD isotherms, respectively. The LM model thus fitted the experimental results more closely than did the FD model in the adsorption of MV. The calculated adsorption capacity is 360.7 mg/g-adsorbent. The results reveal that rh-*g*-PMANa is an excellent adsorbent for MV in water solution. Its adsorption capacity is better than those for nanostructured carbon covered [34], granulated mesoporous carbon [35], and activated palygorskite [36]. rh-*g*-PMANa is a potential adsorbent of MV for wastewater treatment in the textile and painting industries.

3.3.5. Adsorption of MG

Fig. 3(e) plots the adsorption experiment data and the LM and FD correlations of MG. The LM and FD isotherms and their relationship coefficients, *r*, are listed in Table 3. The *r* values are 0.9972 and 0.9938 for LM and FD isotherms, respectively. The LM model thus fitted the experimental results more closely than did the FD model in the adsorption of MG. The calculated monolayer adsorption capacity was 232.8 mg/g-adsorbent. This result is better than those for copper oxide nanoparticle-loaded AC [37], and modified hydroxyapatite [38], but lower than those for tetraethylenepentamine-functionalized AC [39] and magnetic hydroxyapatite nanopowder [40]. However, rh-*g*-PMANa is still a good adsorbent for MG in water solution.

4. Conclusion

A new adsorbent, rh-*g*-PMANa, was prepared via graft copolymerization using Fenton's reagent as a redox initiator. It was shown that rh-*g*-PMANa can be used to adsorb $Pb^{2+}_{(aq)}$, $Cu^{2+}_{(aq)}$, NH_4^+–N, MG, and MV with excellent adsorption capacity in water solution. rh-*g*-PMANa is an environmentally friendly adsorbent and has potential applications for wastewater treatment in many industries.

Acknowledgment

The authors would like to thank Comlets Chemical Industrial Co. Ltd. for supplying raw materials.

References

[1] M. Čehovin, A. Medic, J. Scheideler, J. Mielcke, A. Ried, B. Kompare, A.Ž. Gotvajn, Hydrodynamic cavitation in combination with the ozone, hydrogen peroxide and the UV-based advanced oxidation processes for the removal of natural organic matter from drinking water, Ultrason. Sonochem., 37 (2017) 394–404.
[2] M. Rebhun, N. Galil, Wastewater Treatment Technologies, L. Zirm, J. Mayer, Eds., The Management of Hazardous Substances in the Environment, Elsevier Applied Science, London, 1990, pp. 85–106.
[3] Y. Yureklia, M. Yildirim, L. Aydin, M. Savran, Filtration and removal performances of membrane adsorbers, J. Hazard. Mater., 332 (2017) 33–41.
[4] M.A. Martin-Gonzalez, O. Gonzalez-Diaz, P. Susial, J. Arana, J.A. Herrera-Melian, J.M. Dona-Rodriguez, J. Perez-Pena, Reuse of *Phoenix canariensis* palm frond mulch as biosorbent and as precursor of activated carbons for the adsorption of Imazalil in aqueous phase, Chem. Eng. J., 245 (2014) 348–358.

[5] G. Mezohegyi, F.P. van der Zee, J. Font, A. Fortuny, A. Fabregat, Towards advanced aqueous dye removal processes: a short review on the versatile role of activated carbon, J. Environ. Manage., 102 (2012) 148–164.
[6] M. Plaza-Recobert, G. Trautwein, M. Pérez-Cadenas, J. Alcañiz-Monge, Preparation of binderless activated carbon monoliths from cocoa bean husk, Microporous Mesoporous Mater., 243 (2017) 28–38.
[7] I.A. Aguayo-Villarreal, A. Bonilla-Petriciolet, R. Muñiz-Valencia, Preparation of activated carbons from pecan nutshell and their application in the antagonistic adsorption of heavy metal ions, J. Mol. Liq., 230 (2017) 686–695.
[8] R.H. Hesas, W.M.A.W. Daud, J.N. Sahu, A. Arami-Niya, The effects of a microwave heating method on the production of activated carbon from agricultural waste: a review, J. Anal. Appl. Pyrolysis, 100 (2013) 1–11.
[9] N.A. Medellin-Castillo, R. Ocampo-Pérez, R. Leyva-Ramos, M. Sanchez-Polo, J. Rivera-Utrilla, J.D. Méndez-Díaz, Removal of diethyl phthalate from water solution by adsorption, photo-oxidation, ozonation and advanced oxidation process (UV/H_2O_2, O_3/H_2O_2 and O_3/activated carbon), Sci. Total Environ., 442 (2013) 26–35.
[10] J. Rivera-Utrilla, M. Sanchez-Poloa, V. Gomez-Serranob, P. M. Alvarezc, M.C.M. Alvim-Ferrazd, J.M. Diasd, Activated carbon modifications to enhance its water treatment applications. An overview, J. Hazard. Mater., 187 (2011) 1–23.
[11] S.T. Hsu, T.C. Pan, Adsorption of paraquat using methacrylic acid-modified rice husk, Bioresour. Technol., 98 (2007) 3617–3621.
[12] C.M. Huang, L.C. Chen, H.C. Yang, M.H. Li, T.C. Pan, Preparation of acrylic acid-modified chitin improved by an experimental design and its application in absorbing toxic organic compounds, J. Hazard. Mater., 241–242 (2012) 190–196.
[13] G. Jaria, C.P. Silva, C.I.A. Ferreira, M. Otero, V. Calisto, Sludge from paper mill effluent treatment as raw material to produce carbon adsorbents: an alternative waste management strategy, J. Environ. Manage., 188 (2017) 203–211.
[14] S.A. Opatokun, A. Prabhu, A.A. Shoaibi, C. Srinivasakannan, V. Strezov, Food wastes derived adsorbents for carbon dioxide and benzene gas sorption, Chemosphere, 168 (2017) 326–332.
[15] S.T. Hsu, L.C. Chen, C.C. Lee, T.C. Pan, B.X. You, Q.F. Yan, Preparation of methacrylic acid-modified rice husk improved by an experimental design and application for paraquat adsorption, J. Hazard. Mater., 171 (2009) 465–470.
[16] R. Barbosa, N. Lapa, H. Lopes, A. Gunther, D. Dias, B. Mendes, Biomass fly ashes as low-cost chemical agents for Pb removal from synthetic and industrial wastewaters, J. Colloid Interface Sci., 424 (2014) 27–36.
[17] M.R. Awual, I.M.M. Rahman, T. Yaita, M.A. Khaleque, M. Ferdows, pH dependent Cu(II) and Pd(II) ions detection and removal from aqueous media by an efficient mesoporous adsorbent, Chem. Eng. J., 236 (2014) 100–109.
[18] K.R. Zhu, H. Fu, J.H. Zhang, X.S. Lv, J. Jie Tang, X.H. Xu, Studies on removal of NH^{4+}-N from aqueous solution by using the activated carbons derived from rice husk, Biomass Bioenergy, 43 (2012) 18–25.
[19] J.F. Su, C. Cheng, F. Ma, Comparison of the NH^{4+}-N removal ability by *Klebsiella* sp. FC61 in a bacterial suspension system and a bacterial immobilization system, Sep. Purif. Technol., 172 (2017) 463–472.
[20] A. Mittal, V. Gajbe, J. Mittal, Removal and recovery of hazardous triphenylmethane dye, methyl violet through adsorption over granulated materials, J. Hazard. Mater., 150 (2008) 364–375.
[21] J. Zhang, Y. Li, C.L. Zhang, Y.M. Jing, Adsorption of malachite green from aqueous solution onto carbon prepared from Arundo donax root, J. Hazard. Mater., 150 (2008) 774–782.
[22] S. Agarwal, I. Tyagi, V.K. Gupta, S. Mashhadi, M. Ghasemi, Kinetics and thermodynamics of Malachite Green dye removal from aqueous phase using iron nanoparticles loaded on ash, J. Mol. Liq., 223 (2016) 1340–1347.
[23] J. Li, D.H.L. Ng, P. Song, C. Kong, Y. Song, Synthesis of SnO_2-activated carbon fiber hybrid catalyst for the removal of methyl violet from water, Mater. Sci. Eng., B, 194 (2015) 1–8.
[24] S. Hajati, M. Ghaedi, S. Yaghoubi, Local, cheap and nontoxic activated carbon as efficient adsorbent for the simultaneous removal of cadmium ions and malachite green: optimization by surface response methodology, J. Ind. Eng. Chem., 21 (2015) 760–767.
[25] L. Furlan, V.T. de Fa´vere, M.C.M. Laranjeira, Adsorption of calcium ions by graft copolymer of acrylic acid on biopolymer chitin, Polymer, 37 (1996) 843–846.
[26] S. Tiwari, A. Hasan, L.M. Pandey, A novel bio-sorbent comprising encapsulated *Agrobacterium fabrum* (SLAJ731) and iron oxide nanoparticles for removal of crude oil co-contaminant, lead Pb(II), J. Environ. Chem. Eng., 5 (2017) 442–452.
[27] D. Sasmal, J. Maity, H. Kolya, T. Tripathy, Selective adsorption of Pb (II) ions by amylopectin-g-poly(acrylamide-co-acrylic acid): a bio-degradable graft copolymer, Int. J. Biol. Macromol., 97 (2017) 585–597.
[28] K.A. Gebru, C. Das, Removal of Pb (II) and Cu (II) ions from wastewater using composite electrospun cellulose acetate/titanium oxide (TiO_2) adsorbent, J. Water Process Eng., 16 (2017) 1–13.
[29] M. Kong, H. Song, F. Li, D. Dai, H. Gao, Facile synthesis of $Bi_2Fe_4O_9$ nanoplate and its application as a novel adsorbent for Cu(II) removal, J. Environ. Chem. Eng., 5 (2017) 69–78.
[30] C.W. Xaio, X.J. Liu, S.M. Mao, L.J. Zhang, J. Lu, Sub-micron-sized polyethylenimine-modified polystyrene/Fe_3O_4/chitosan magnetic composites for the efficient and recyclable adsorption of Cu(II) ions, Appl. Surf. Sci., 394 (2017) 378–385.
[31] T.H. Martins, T.S.O. Souza, E. Foresti, Ammonium removal from landfill leachate by Clinoptilolite adsorption followed by bioregeneration, J. Environ. Chem. Eng., 5 (2017) 63–68.
[32] Z.H. Wang, H.Y. Guo, F. Shen, G. Yang, Y.Z. Zhang, Y.M. Zeng, L.L. Wang, H. Xiao, S.H. Deng, Biochar produced from oak sawdust by Lanthanum (La)-involved pyrolysis for adsorption of ammonium (NH_4^+), nitrate (NO_3^-), and phosphate (PO_4^{3-}), Chemosphere, 119 (2015) 646–653.
[33] X.G. Wang, S.Y. Lu, C.M. Gao, X.B. Xu, X.J. Zhang, X. Bai, M.Z. Liu, L. Wu, Highly efficient adsorption of ammonium onto palygorskite nanocomposite and evaluation of its recovery as a multifunctional slow-release fertilizer, Chem. Eng. J., 252 (2014) 404–414.
[34] S. Moradi, S. Azizian, Preparation of nanostructured carbon covered sand for removal of methyl violet from water, J. Mol. Liq., 219 (2016) 909–913.
[35] Y. Kim, J. Bae, H. Park, J.K. Suh, Y.W. You, H. Choi, Adsorption dynamics of methyl violet onto granulated mesoporous carbon: facile synthesis and adsorption kinetics, Water Res., 101 (2016) 187–194.
[36] G.Y. Tian, W.B. Wang, Y.R. Kang, A.Q. Wang, Ammonium sulfide-assisted hydrothermal activation of palygorskite for enhanced adsorption of methyl violet, J. Environ. Sci., 41 (2016) 33–43.
[37] E.A. Dil, M. Ghaedi, A. Asfaram, S. Hajati, F. Mehrabi, A. Goudarzi, Preparation of nanomaterials for the ultrasound-enhanced removal of Pb^{2+} ions and malachite green dye: chemometric optimization and modeling, Ultrason. Sonochem., 34 (2017) 677–691.
[38] A.A. El-Zahhar, N.S. Awwad, Removal of malachite green dye from aqueous solutions using organically modified hydroxyapatite, J. Environ. Chem. Eng., 4 (2016) 633–638.
[39] M. Ghasemi, S. Mashhadi, M. Asif, I. Tyagi, S. Agarwal, V.K. Gupta, Microwave-assisted synthesis of tetraethylenepentamine functionalized activated carbon with high adsorption capacity for Malachite green dye, J. Mol. Liq., 213 (2016) 317–325.
[40] F. Zhang, B.L. Ma, X.P. Jiang, Y.F. Ji, Dual function magnetic hydroxyapatite nanopowder for removal of malachite green and Congo red from aqueous solution, Powder Technol., 302 (2016) 207–214.

Supplementary figures

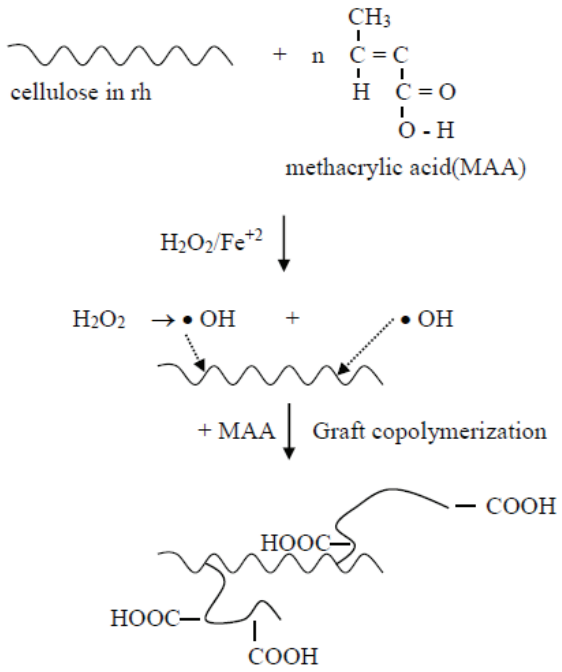

Fig. S1. Reaction scheme of the copolymerization of MAA and rice husk.

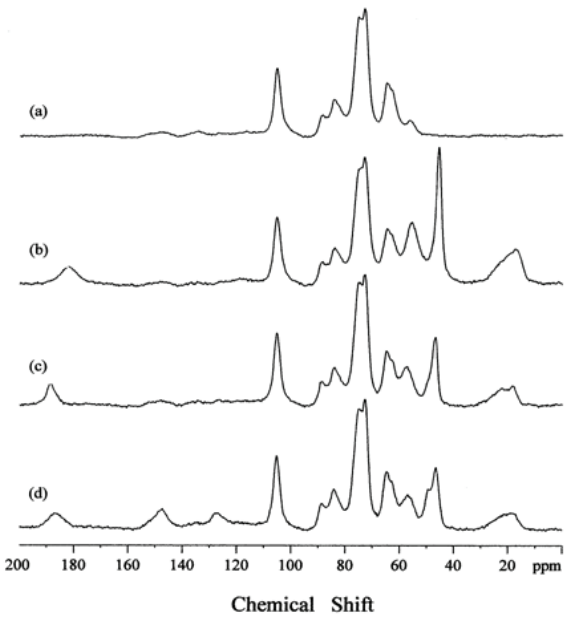

Fig. S2. Solid-state 13C NMR spectra of (a) rice husk, (b) graft copolymer of PMAA and rice husk, (c) hydrolyzed copolymer, and (d) hydrolyzed copolymer after adsorption of paraquat [15].